CrystEngComm

COMMUNICATION

View Article Online
View Journal | View Issue

Cite this: *CrystEngComm*, 2016, **18**, 8829

Received 5th September 2016,
Accepted 18th October 2016

DOI: 10.1039/c6ce01939k

www.rsc.org/crystengcomm

Influence of intra-skeletal coral lipids on calcium carbonate precipitation†‡

M. Reggi,[a] S. Fermani,[a] C. Samorì,[ab] F. Gizzi,[c] F. Prada,[c] Z. Dubinsky,[d] S. Goffredo*[c] and G. Falini*[a]

Recent research studies have shown that the intra-skeletal organic matrix of corals contains lipids. This communication reports their characterization and their influence on calcium carbonate precipitation. In addition, their potential role in coral's biomineralization is discussed.

Biomineralization in corals takes place at the interface between the aboral epidermis, called the calicoblastic epithelium, and the aragonitic skeleton underneath.[1] The material between these two tissues constitutes the extracellular calcifying matrix (ECM),[1] and is a highly viscous sol composed of adhesive glycoproteins and proteoglycans. In the ECM, biological macromolecules, called the organic matrix (OM), are secreted from the calicoblastic epithelium.[2] The release of OM components is orchestrated by the organisms in space and time.[3–8] The structure and function of the intra-skeletal OM of scleractinian corals have been investigated in detail in *in vivo* and *in vitro* systems. These studies have provided insight into the fundamental role of the intraskeletal OM in controlling the calcification process.[1,3,4,8–11]

The OM composition varies with the coral taxon[12,13] and is species specific,[9,11] but exhibits common chemical features. They are the presence of acidic glycoproteins having carboxylated residues,[14] polysaccharides often functionalized with sulphate groups,[15,16] and lipids.[17] So far the research has mainly focused on the acidic glycoproteins because it has been recognized that acidic proteins and peptides control calcium carbonate ($CaCO_3$) deposition providing specific structural arrays for the recognition and binding of crystalline planes.[15,18–21] The influence of the OM lipids (*lip*OM) on the precipitation of $CaCO_3$ has not been investigated. This is despite the fact that lipids are components not only of the OM of corals, but also of several molluscs.[22] In corals, lipids are mainly associated with soft tissue and are structural components of cell membranes and signal molecules.[23] Their content varies between different species according to their lipogenetic pathways and can be affected by environmental conditions and the coral's diet.[24] However, their presence in the OM may invoke a role at some stage in the calcification process. Lipids are present in the OM as free fatty acids (FA) and, in lesser amounts, phospholipids, sterols, ceramids and sterol esters.[17] Isa and Okazaki[25] showed that phospholipids extracted from the skeleton of scleractinian are able to bind calcium, and therefore suggested that they can serve as nucleation sites for the deposition of $CaCO_3$.

In addition, it has been widely shown that lipids affect the *in vitro* $CaCO_3$ formation.[17] Phospholipids stabilized the precipitation of the transient amorphous calcium carbonate (ACC) before crystalline phases through the interaction with phosphate groups.[26,27]

Herein, the influence of *lip*OM on $CaCO_3$ precipitation *in vitro* was investigated. The *lip*OM were extracted from the coral species, *Astroides calycularis*, *Balanophyllia europaea* and *Stylophora pistillata*. These species are representative of a diverse trophic strategy and growth forms.[1,28]

The samples of *B. europaea*, *A. calycularis* from Palinuro (Italian coast, North-Western Mediterranean Sea) and *S. pistillata* from the Gulf of Eilat (Red Sea, Israel) were collected by scuba diving. The *lip*OM were extracted from the

[a] *Dipartimento di Chimica "Giacomo Ciamician", Alma Mater Studiorum - Università di Bologna, via Selmi 2, 40126 Bologna, Italy. E-mail: giuseppe.falini@unibo.it*
[b] *Centro Interdipartimentale di Ricerca in Scienze Ambientali, Sede di Ravenna - Università di Bologna, via S. Alberto 163, 48100 Ravenna, Italy*
[c] *Marine Science Group, Department of Biological, Geological and Environmental Sciences, Alma Mater Studiorum - Università di Bologna, Via Selmi 3, I-40126 Bologna, Italy*
[d] *The Mina & Everard Goodman Faculty of Life Sciences, Bar-Ilan University, Ramat-Gan 5290002, Israel*

† Electronic supplementary information (ESI) available: Materials and methods; Table ESI1, Fig. ESI1–4. See DOI: 10.1039/c6ce01939k

‡ This work has received funding from the European Research Council under the European Union's Seventh Framework Programme (FP7/2007–2013)/ERC Grant Agreement No. [249930 – CoralWarm: Corals and global warming: the Mediterranean *versus* the Red Sea]. GF and SF thank the CIRCMSB for the support.

whole intra-skeletal organic matrix (*w*OM; *i.e.*, soluble and insoluble fractions) and characterized (details in the ESI†). Then, *lip*OM were dispersed (100 μg mL^{-1}) in a 10 mM $CaCl_2$ solution by sonication and their assembly was analysed (see ESI†). The $CaCO_3$ precipitation trials were carried out using the vapour diffusion method (details in the ESI†). Precipitates were characterized by FTIR spectroscopy and microscopic observations.

The content of *lip*OM was always around 0.1 wt% with respect to the mass of the skeleton (Table 1). *A. calycularis* was the species with the lowest lipid content (0.7 ± 0.5‰), while *S. pistillata* (1.1 ± 0.8‰) and *B. europaea* (1.0 ± 0.35‰) showed a similar content of lipids. The absence of the symbiotic zooxanthellae, which biosynthesize lipids, in *A. calycularis* could justify this observation.

The first characterization of *lip*OM was performed by FTIR spectroscopy. Fig. 1 shows the most representative spectra of *lip*OM for each species where small differences in absorption profiles were recorded among samples from the same species. A description of the assigned absorption bands is listed in Table ESI1.†

The relative intensities of these bands changed according to the *lip*OM source. The spectra from *A. calycularis* and *B. europaea* showed the most intense bands due to FA (2851–2956 cm^{-1}), namely the vibration modes associated with methylene and methyl groups. This preponderance was less marked in the *lip*OM from *S. pistillata*. The *lip*OM from *A. calycularis* and *B. europaea* also showed a strong signal for bonds between FA and glycerol (1735 cm^{-1}), which can be considered as an index of the presence of triglycerides and phospholipids. The latter was in low relative quantities due to the weak absorption of the bands associated with the phosphate group (1026 cm^{-1}). The FTIR spectrum of *lip*OM from *S. pistillata* indicates the presence of ceramids and glycolipids (bands around 1643 cm^{-1}) with a high degree of methylation (1384 cm^{-1}). These differences in *lip*OM can be associated with different lipogenesis pathways among organisms and a diverse uptake of lipids from the organism's surrounding environment.

The FA components of the *lip*OM were analysed by gas chromatography-mass spectrometry (Table 1), which revealed that palmitic acid (16 : 0) was the most abundant FA, followed by stearic (18 : 0) in order of concentration. Oleic acid (18 : 1) was detected as the third main component. The distribution of these components was quite equal among the diverse coral species.

Table 1 Content (wt%) and composition (wt%) of FA extracted from the coral skeleton from *A. calycularis* (ACL), *B. europaea* (BEU) and *S. pistillata* (SPT). When the sum of the percentages was not 100, some unassigned FA was found to be present. The standard deviation is reported

FA	ACL	BEU	SPT
Content	0.7 ± 0.5	1.0 ± 0.5	1.1 ± 0.8
Composition			
C14:0	3.9 ± 0.9	6.1 ± 2.4	2.6 ± 0.7
C15:0	4.5 ± 2.7		
C16:0	51.0 ± 2.6	52.4 ± 1.6	47.5 ± 1.3
C17:0	4.6 ± 0.6		
C18:1	—	14.7 ± 1.6	8.1 ± 3.2
C18:0	42.6 ± 1.8	29.5 ± 1.7	41.8 ± 1.5

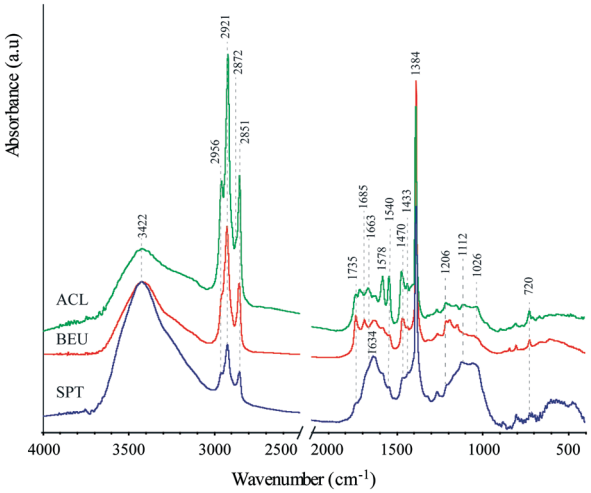

Fig. 1 FTIR spectra of intra-skeletal lipidic components of the organic matrix extracted from the skeleton of *A. calycularis* (ACL), *B. europaea* (BEU), and *S. pistillata* (SPT). The wavenumber of the main absorption bands are indicated.

*Lip*OM, only when dispersed at a concentration of 100 μg mL^{-1} in the 10 mM $CaCl_2$, assembled in particles having hydrodynamic radii of 239.5 ± 7.4 nm and 232.5 ± 7.1 nm for *A. calycularis* and *S. pistillata*, respectively, and of 169.9 ± 6.7 nm for *B. europaea*. These diverse values have to be related to the *lip*OM composition that affects the calcium ions mediated process of assembly.

The influence of the *lip*OM assembled particles on $CaCO_3$ precipitation was evaluated by comparison with experiments in the presence of the *w*OM (in a concentration equal to that of *w*OM from which *lip*OM was extracted) and in the absence of additives. In the absence of additives, only rhombohedral calcite crystals were formed (Fig. ESI1†). The presence of *w*OM inhibited the precipitation of $CaCO_3$ and less precipitates formed with respect to the control (Fig. ESI2†), as already reported.[3] The FTIR spectra showed that in these experiments only calcite was formed (Fig. ESI3†). The *w*OM from *A. calycularis* and *B. europaea* (Fig. 2 ACL and BEU) provoked the precipitation of agglomerates and aggregates of modified calcite rhombohedric crystals on the insoluble fraction of the *w*OM (Fig. 2).

In the presence of *S. pistillata*, *w*OM aggregates developed a spherical shape and embedded the insoluble *w*OM (Fig. 2 SPT). More images are available in Fig. ESI4.†

In the presence of *lip*OM, $CaCO_3$ precipitation was inhibited even to a higher extent than that in the presence of *w*OM (Fig. ESI2†). Calcite and small amounts of vaterite precipitated in the presence of *lip*OM from *A. calycularis* and *B. europaea*. However, in the presence of *lip*OM from *S. pistillata*, only calcite precipitated as noted by the diagnostic absorption band at 712 cm^{-1} and 744 cm^{-1} of calcite and vaterite, respectively, in the FTIR spectra (Fig. ESI3†). The

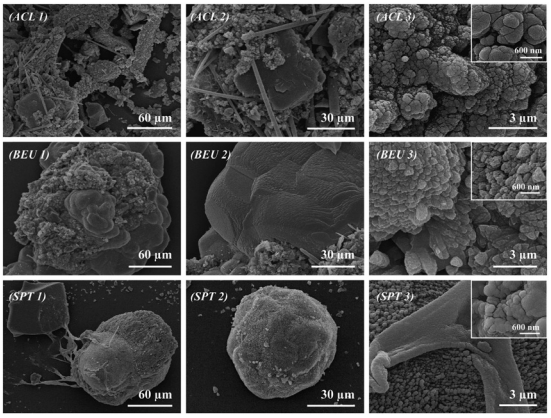

Fig. 2 Scanning electron microscopy pictures at increasing magnification (1–3) of crystals obtained from *in vitro* $CaCO_3$ crystallization experiments from a 10 mM $CaCl_2$ solution in the presence of *w*OM extracted from *A. calycularis* (ACL), *B. europaea* (BEU) and *S. pistillata* (SPT). In column 3, the particles that covered the *w*OMs surface are shown. In the insets, high magnification images are shown with the granular submicrometer particles from the surface of the crystal. These pictures show the most representative particles of each population.

majority of these particles appeared as modified rhombohedral single crystals and a few of them were polycrystalline aggregates (Fig. 3). The size of the single crystals was in the range of 10–35 μm in the presence of *lip*OM from *S. pistillata*, smaller than those formed in the presence of *lip*OM from *A. calycularis* (14–74 μm) or *B. europaea* (27–62 μm). The presence of *lip*OM from *S. pistillata* generated an affected morphology, in which specific {*hk*0} crystalline faces were stabilized. On the contrary, in the presence of *lip*OM from *A. calycularis* or *B. europaea*, the crystals were not particularly affected in their morphology and {*hkl*} crystalline faces appeared. Most importantly, a clear marker for the presence of *lip*OM was the presence of cavities and pores on the crystals' surfaces. This effect was particularly marked for *S. pistillata* (Fig. 3, column 3). These pores had sizes that were certain orders of magnitude higher than the hydrodynamic radii of the *lip*OM particles measured in the presence of calcium ions. Thus, an aggregation of *lip*OM particles during the $CaCO_3$ precipitation process is likely. In addition to this observation, the high magnification images of the crystal surfaces showed that the spheroidal calcitic grains forming the crystal were not compact (Fig. 3, column 3), as observed in the presence of the *w*OM (Fig. 2, insets). The presence of pores on the calcite crystals was the most remarkable effect of the presence of the *lip*OM. This effect is a consequence of the capability of the *lip*OM to assemble in particles in the presence of calcium ions, an effect observed using pseudo peptides and lecitins.[29,30] When *w*OM was used, pores were not observed on the surface of $CaCO_3$ particles, suggesting that in the *w*OM the lipids had diverse ultra-structure organizations with respects to those in the *lip*OM, making them unable to generate pores. The extraction of lipids from *w*OM did not change the *w*OM way to affect the crystallization of $CaCO_3$ (data not reported).

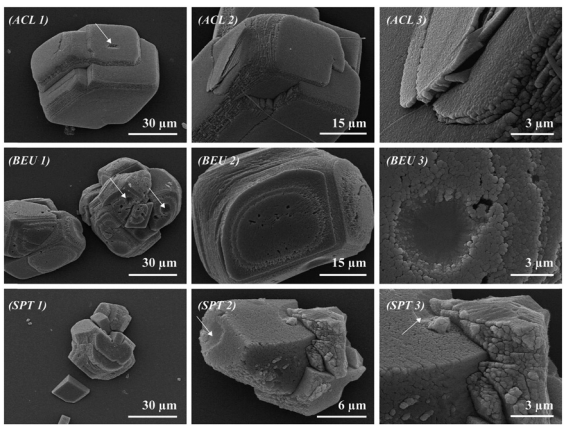

Fig. 3 Scanning electron microscopy pictures at increasing magnification (1–3) of crystals obtained from *in vitro* $CaCO_3$ crystallization experiments from 10 mM $CaCl_2$ solution where *lip*OMs from *A. calycularis* (ACL), *B. europaea* (BEU) and *S. pistillata* (SPT) were dispersed. The arrows indicate some dips on the surface of crystals. These pictures show the most representative particles of each population.

Thus, the aggregated status of *lip*OM in particles, when calcium ions are present, is a key parameter to obtain pores on calcite. This capability could have biological implications by affecting coral micro-density and mechanical properties, although corals biomineralize aragonite and not calcite.[1] The coral micro-density is 2.55, 2.73 and 2.63 mg mm^{-3} for *A. calycularis*,[31] *B. europaea*[32] and *S. pistillata*,[31] respectively. The difference in micro-density with that of pure inorganic aragonite, 2.94 mg mm^{-3},[33] cannot be justified only by the presence of the *w*OM. The latter, supposing a density of 1.3 mg mm^{-3},[34] should represent a content of about 12, 6 and 9 wt%, for *A. calycularis*, *B. europaea* and *S. pistillata*, respectively; this disagrees with experimental data, showing a content of *w*OM equal to 2.7 ± 0.1,[35] 2.9 ± 0.1 (ref. 35) and no more than 2 wt%,[36] respectively. According to these data, to justify the measured micro-density, a mass around 9.2, 3.2 and 7.3 wt% for the abovementioned species, respectively, of the skeleton should not be occupied by aragonite and *w*OM materials, probably water solutions or lower density mineral phases (*e.g.* ACC[37]). This mass will occupy a volume of the skeleton, which can range from 18, 7 and 15 vol% (considering it equivalent to *w*OM) to 8, 3 and 6 vol% (considering it equivalent to aragonite) for *A. calycularis*, *B. europaea* and *S. pistillata*, respectively. This agrees with the microscopic observations of Benzerara *et al.*[38] who reported an extended porosity in the skeleton, even if not quantified. This was localized among the mineral grains of the center of calcification and within the aragonitic fibres. The formation of these pores, according to our *in vitro* experimental data, is favoured by molecular assemblies that lipids form in the presence of calcium ions and their subsequent entrapment within the skeleton structure.

The entrapment of particle additives and the generation of porosity within $CaCO_3$ have been widely reported for synthetic hybrid calcite crystals. Monodispersed copolymer latex particles functionalized by carboxylate groups were used to

obtain calcite crystals with a rhombohedral morphology and uniform surface pores by a three-step mechanism.[39] Single crystals of calcite were occluded with 13 wt% of 20 nm anionic diblock copolymer micelles, which were specifically adsorbed on {104} faces and changed shape upon incorporation within the crystal lattice.[40]

In the *in vivo* system, the organism controls in space and time the release of lipids, as of other OM components. Thus the *lip*OM could have some additional functional roles. In corals, ion transport through the epithelial layers is reported to occur by means of two pathways: a paracellular pathway driven by diffusion/seawater flow or a transcellular pathway driven by active/facilitated transport or both. A third mechanism could involve the vesicle-confined space (syncytium) and the formation of calcification elements within a vesicle, as reported for molluscs and foraminifera.[11] In the latter, the lipids form vesicles in which the medium from which the ions are derived (seawater or body fluids) is confined. Once these vesicles are released, the calcification elements could be entrapped by the growing skeleton contributing to the generation of porosity.

Conclusions

This research has shown that the intra-skeletal lipids of corals are able to generate an *in vitro* porosity in the crystals of calcite. This observation has relevance in the understanding of the coral biomineralization process and in justifying the coral micro-density.

Notes and references

1 S. Tambutte, M. Holcomb, C. Ferrier-Pages, S. Reynaud, E. Tambutte, D. Zoccola and D. Allemand, *J. Exp. Mar. Biol. Ecol.*, 2011, **408**, 58–78.
2 L. Muscatine, C. Goiran, L. Land, J. Jaubert, J. P. Cuif and D. Allemand, *Proc. Natl. Acad. Sci. U. S. A.*, 2005, **102**, 1525–1530.
3 Y. Dauphin, J.-P. Cuif and C. T. Williams, *Comp. Biochem. Physiol., Part B: Biochem. Mol. Biol.*, 2008, **150**, 10–22.
4 Y. Dauphin, *Int. J. Biol. Macromol.*, 2001, **28**, 293–304.
5 J. P. Cuif and Y. Dauphin, *J. Struct. Biol.*, 2005, **150**, 319–331.
6 J. P. Cuif, Y. Dauphin, J. Doucet, M. Salome and J. Susini, *Geochim. Cosmochim. Acta*, 2003, **67**, 75–83.
7 T. Watanabe, I. Fukuda, K. China and Y. Isa, *Comp. Biochem. Physiol., Part B: Biochem. Mol. Biol.*, 2003, **136**, 767–774.
8 S. Puverel, E. Tambutte, L. Pererra-Mouries, D. Zoccola, D. Allemand and S. Tambutte, *Comp. Biochem. Physiol., Part B: Biochem. Mol. Biol.*, 2005, **141**, 480–487.
9 M. Reggi, S. Fermani, V. Landi, F. Sparla, E. Caroselli, F. Gizzi, Z. Dubinsky, O. Levy, J.-P. Cuif, Y. Dauphin, S. Goffredo and G. Falini, *Cryst. Growth Des.*, 2014, **14**, 4310–4320.
10 G. Falini, M. Reggi, S. Fermani, F. Sparla, S. Goffredo, Z. Dubinsky, O. Levi, Y. Dauphin and J.-P. Cuif, *J. Struct. Biol.*, 2013, **183**, 226–238.
11 S. Weiner and L. Addadi, *Annu. Rev. Mater. Res.*, 2011, **41**, 21–40.
12 P. M. Dove, *Elements*, 2010, **6**, 37–42.
13 J. P. Cuif, Y. Dauphin, A. Freiwald, P. Gautret and H. Zibrowius, *Comp. Biochem. Physiol., Part A: Mol. Integr. Physiol.*, 1999, **123**, 269–278.
14 S. Weiner, W. Traub and H. A. Lowenstam, in *Biomineralization and Biological Metal Accumulation*, ed. P. Westbroek and E. W. de Jong, Springer Netherlands, 1983, pp. 205–224.
15 S. Albeck, S. Weiner and L. Addadi, *Chem. – Eur. J.*, 1996, **2**, 278–284.
16 J. L. Arias and M. S. Fernandez, *Chem. Rev.*, 2008, **108**, 4475–4482.
17 B. Farre, J. P. Cuif and Y. Dauphin, *Zoology*, 2010, **113**, 250–257.
18 S. Weiner and L. Addadi, *J. Mater. Chem.*, 1997, **7**, 689–702.
19 L. Addadi, J. Moradian, E. Shay, N. G. Maroudas and S. Weiner, *Proc. Natl. Acad. Sci. U. S. A.*, 1987, **84**, 2732–2736.
20 R. M. Mitterer, *Bull. Mar. Sci.*, 1978, **28**, 173–180.
21 G. K. Hunter, *Curr. Opin. Solid State Mater. Sci.*, 1996, **1**, 430–435.
22 B. Farre and Y. Dauphin, *Comp. Biochem. Physiol. B*, 2008, **152**, 103–109.
23 J. S. Stimson, *Bull. Mar. Sci.*, 1987, **41**, 889–904.
24 A. B. Imbs, N. A. Latyshev, N. W. Zhukova and T. N. Dautova, *Comp. Biochem. Physiol., Part B: Biochem. Mol. Biol.*, 2007, **148**, 314–321.
25 Y. Isa and M. Okazaki, *Comp. Biochem. Physiol., Part B: Biochem. Mol. Biol.*, 1987, **87**, 507–512.
26 J. P. Cuif, Y. Dauphin, P. Berthet and J. Jegoudez, *Geochem., Geophys., Geosyst.*, 2004, **5**, 11.
27 C. C. Tester, R. E. Brock, C. H. Wu, M. R. Krejci, S. Weigand and D. Joester, *CrystEngComm*, 2011, **13**, 3975–3978.
28 A. Adamiano, S. Goffredo, Z. Dubinsky, O. Levy, S. Fermani, D. Fabbri and G. Falini, *Anal. Bioanal. Chem.*, 2014, **406**, 6021–6033.
29 C. Tomasini, N. Castellucci, V. C. Caputo, L. Milli, G. Battistelli, S. Fermani and G. Falini, *CrystEngComm*, 2015, **17**, 116–123.
30 C. Beato, M. S. Fernandez, S. Fermani, M. Reggi, A. Neira-Carrillo, A. Rao, G. Falini and J. L. Arias, *CrystEngComm*, 2015, **17**, 5953–5961.
31 F. Prada and E. Caroselli, personnel communication.
32 E. Caroselli, F. Prada, L. Pasquini, F. N. Marzano, F. Zaccanti, G. Falini, O. Levy, Z. Dubinsky and S. Goffredo, *Zoology*, 2011, **114**, 255–264.
33 D. S. Marszalek, *Mar. Behav. Physiol.*, 1982, **8**, 295–303.
34 E. T. White, W. H. Tan, J. M. Ang, S. Tait and J. D. Litster, *Powder Technol.*, 2007, **179**, 55–58.
35 G. Falini, S. Fermani and S. Goffredo, *Semin. Cell Dev. Biol.*, 2015, **46**, 17–26.
36 E. Tambutte, A. A. Venn, M. Holcomb, N. Segonds, N. Techer, D. Zoccola, D. Allemand and S. Tambutte, *Nat. Commun.*, 2015, 6.

37 L. Brečević and A. E. Nielsen, *J. Cryst. Growth*, 1989, **98**, 504–510.
38 K. Benzerara, N. Menguy, M. Obst, J. Stolarski, M. Mazur, T. Tylisczak, G. E. Brown Jr and A. Meibom, *Ultramicroscopy*, 2011, **111**, 1268–1275.
39 C. Lu, L. Qi, H. Cong, X. Wang, J. Yang, L. Yang, D. Zhang, J. Ma and W. Cao, *Chem. Mater.*, 2005, **17**, 5218–5224.
40 Y.-Y. Kim, K. Ganesan, P. Yang, A. N. Kulak, S. Borukhin, S. Pechook, L. Ribeiro, R. Kröger, S. J. Eichhorn, S. P. Armes, B. Pokroy and F. C. Meldrum, *Nat. Mater.*, 2011, **10**, 890–896.